University Library

MINERVA ACCESS

A gateway to Melbourne's research publications

Minerva Access is the Institutional Repository of The University of Melbourne

Author/s:
Correia, JC;Jannig, PR;Gosztyla, ML;Cervenka, I;Ducommun, S;Præstholm, SM;Dias, JM;Dumont, KD;Liu, Z;Liang, Q;Edsgärd, D;Emanuelsson, O;Gregorevic, P;Westerblad, H;Venckunas, T;Brazaitis, M;Kamandulis, S;Lanner, JT;Teixeira, AI;Yeo, GW;Ruas, JL

Title:
Zfp697 is an RNA-binding protein that regulates skeletal muscle inflammation and remodeling

Date:
2024

Citation:
Correia, J. C., Jannig, P. R., Gosztyla, M. L., Cervenka, I., Ducommun, S., Præstholm, S. M., Dias, J. M., Dumont, K. D., Liu, Z., Liang, Q., Edsgärd, D., Emanuelsson, O., Gregorevic, P., Westerblad, H., Venckunas, T., Brazaitis, M., Kamandulis, S., Lanner, J. T., Teixeira, A. I. ,... Ruas, J. L. (2024). Zfp697 is an RNA-binding protein that regulates skeletal muscle inflammation and remodeling. Proceedings of the National Academy of Sciences of the United States of America, 121 (34), https://doi.org/10.1073/pnas.2319724121.

Persistent Link:
https://hdl.handle.net/11343/358439

License:
CC BY-NC-ND

PNAS RESEARCH ARTICLE | PHYSIOLOGY

Zfp697 is an RNA-binding protein that regulates skeletal muscle inflammation and remodeling

Jorge C. Correia[a], Paulo R. Jannig[a], Maya L. Gosztyla[b,c,d], Igor Cervenka[a], Serge Ducommun[a], Stine M. Præstholm[a], José M. Dias[e,f], Kyle D. Dumont[a], Zhengye Liu[g], Qishan Liang[b,d,h], Daniel Edsgärd[i], Olof Emanuelsson[i], Paul Gregorevic[j], Håkan Westerblad[k], Tomas Venckunas[l], Marius Brazaitis[l], Sigitas Kamandulis[l], Johanna T. Lanner[g], Ana I. Teixeira[e], Gene W. Yeo[b,c,d], and Jorge L. Ruas[a,m,1]

Affiliations are included on p. 10.

Edited by Christoph Handschin, Universitat Basel, Basel, Switzerland; received November 17, 2023; accepted June 27, 2024 by Editorial Board Member David J. Mangelsdorf

Skeletal muscle atrophy is a morbidity and mortality risk factor that happens with disuse, chronic disease, and aging. The tissue remodeling that happens during recovery from atrophy or injury involves changes in different cell types such as muscle fibers, and satellite and immune cells. Here, we show that the previously uncharacterized gene and protein Zfp697 is a damage-induced regulator of muscle remodeling. Zfp697/ZNF697 expression is transiently elevated during recovery from muscle atrophy or injury in mice and humans. Sustained Zfp697 expression in mouse muscle leads to a gene expression signature of chemokine secretion, immune cell recruitment, and extracellular matrix remodeling. Notably, although Zfp697 is expressed in several cell types in skeletal muscle, myofiber-specific Zfp697 genetic ablation in mice is sufficient to hinder the inflammatory and regenerative response to muscle injury, compromising functional recovery. We show that Zfp697 is an essential mediator of the interferon gamma response in muscle cells and that it functions primarily as an RNA-interacting protein, with a very high number of miRNA targets. This work identifies Zfp697 as an integrator of cell–cell communication necessary for tissue remodeling and regeneration.

skeletal muscle | Zfp697 | muscle atrophy | inflammation | RNA-binding protein

Significance

We identify Zfp697 as a critical regulator of the inflammatory and regenerative response to skeletal muscle injury. Zfp697 ablation in mouse muscle fibers impairs functional recovery from injury-related challenges, highlighting the central role of this mechanism in tissue remodeling and regeneration. We show that Zfp697 is a novel RNA-binding protein and a critical mediator of the inflammatory response to interferon gamma (IFNγ). Notably, Zfp697 is expressed in numerous cell types beyond skeletal muscle and genetic variants in the ZNF697 genomic locus have been associated with the response of multiple sclerosis patients to IFNβ treatment. Given the pleiotropic effects of interferons on immunity, antiviral response, and tumorigenesis, this mechanism is likely to have implications in other tissues and biological contexts.

Skeletal muscle accounts for ca. 40% of the total body mass of a lean individual and is fundamental for breathing, posture, and locomotion. It also plays a crucial role in the regulation of energy metabolism and temperature and has important endocrine functions (1). Skeletal muscle mass and function are associated with overall quality of life and health and are inversely correlated with the risk of death. Skeletal muscle is quantitatively and qualitatively responsive to use and disuse changing its mass, metabolism, and fiber size and type accordingly (2). Both muscle regeneration and hypertrophy depend on changes in fiber protein turnover and autophagy, and on several cell types that include satellite cells, fibro-adipogenic progenitors, and immune cells (3, 4). Perturbations in any of these components will affect recovery from muscle atrophy by compromising regeneration and hypertrophy. Indeed, it has been shown that failure to recruit immune cells such as neutrophils, macrophages, and T cells compromises muscle repair and growth (5, 6). Accordingly, several cytokines and chemokines have been involved in mediating the cell–cell communication processes necessary for tissue repair. Last, remodeling the extracellular matrix (ECM) is necessary to create the right tissue environment and structure to support and transduce force generated by regenerating fibers or as they become larger and stronger. As dependent as muscle regeneration and hypertrophy are on these inflammatory and remodeling processes, failure to resolve them results in tissue fibrosis and progressive loss of function (7). This is often seen in muscular dystrophies, where constant tissue injury created by fiber fragility promotes exacerbated immune cell infiltration, permanent tissue inflammation, and excessive ECM deposition and remodeling (8). Understanding how these processes are regulated has important implications for clinical and space medicine and will pave the way for the development of therapies for muscle injury, trauma, recovery from intense exercise, and muscle genetic diseases. Indeed, our understanding of the molecular mechanisms that govern muscle transition from eutrophy to atrophy is more complete than of those that regulate recovery. In this study, we aimed to identify genes and molecular pathways relevant for the regulation of skeletal muscle plasticity. Here, we uncover the role of the previously uncharacterized zinc finger protein 697 (Zfp697 in mice and ZNF697 in humans) as a central regulator of muscle inflammation, remodeling, and compensatory hypertrophy. We show that Zfp697 expression is transiently increased in situations of intense exercise, muscle injury, or recovery from atrophy. When induced, Zfp697 promotes the expression of genes involved in immune

Competing interest statement: G.W.Y. is an Scientific Advisory Board (SAB) member of Jumpcode Genomics and a co-founder, member of the Board of Directors, on the SAB, equity holder, and paid consultant for Locanabio and Eclipse BioInnovations. G.W.Y. is a distinguished visiting professor at the National University of Singapore. G.W.Y.'s interests have been reviewed and approved by the University of California, San Diego in accordance with its conflict-of-interest policies.

This article is a PNAS Direct Submission. C.H. is a guest editor invited by the Editorial Board.

Copyright © 2024 the Author(s). Published by PNAS. This article is distributed under Creative Commons Attribution-NonCommercial-NoDerivatives License 4.0 (CC BY-NC-ND).

[1]To whom correspondence may be addressed. Email: jlruas@med.umich.edu.

This article contains supporting information online at https://www.pnas.org/lookup/suppl/doi:10.1073/pnas.2319724121/-/DCSupplemental.

Published August 14, 2024.

cell recruitment, satellite cell activation, and ECM remodeling. Loss of Zfp697 expression in the muscle fiber by genetic deletion severely compromises muscle repair, force recovery, and function. Conversely, prolonged Zfp697 expression leads to tissue inflammation and fibrosis. In addition, we explore the mechanism of Zfp697 action and regulation by upstream stimuli and identify a critical role in transducing the regenerative actions of interferon gamma (IFNγ) in muscle. Importantly, Zfp697 is expressed in several other tissues, including the kidney and heart, where unresolved inflammation and fibrosis are common disease hallmarks. This positions Zfp697 as potential therapeutic target for several pathologies.

Results

Zfp697 Expression Is Induced during Skeletal Muscle Recovery from Atrophy or Injury. To identify molecular mechanisms that control skeletal muscle remodeling, such as those that regulate the transition from atrophy to compensatory hypertrophy, we used a mouse model of hindlimb unloading/reloading (Fig. 1*A*) (9, 10). This protocol resulted in approximately 30% reduction in gastrocnemius mass after 10 d of unloading, which required more than 7 d of reloading to recover to control levels (Fig. 1*B*). To identify gene regulatory events taking place upon muscle reloading,

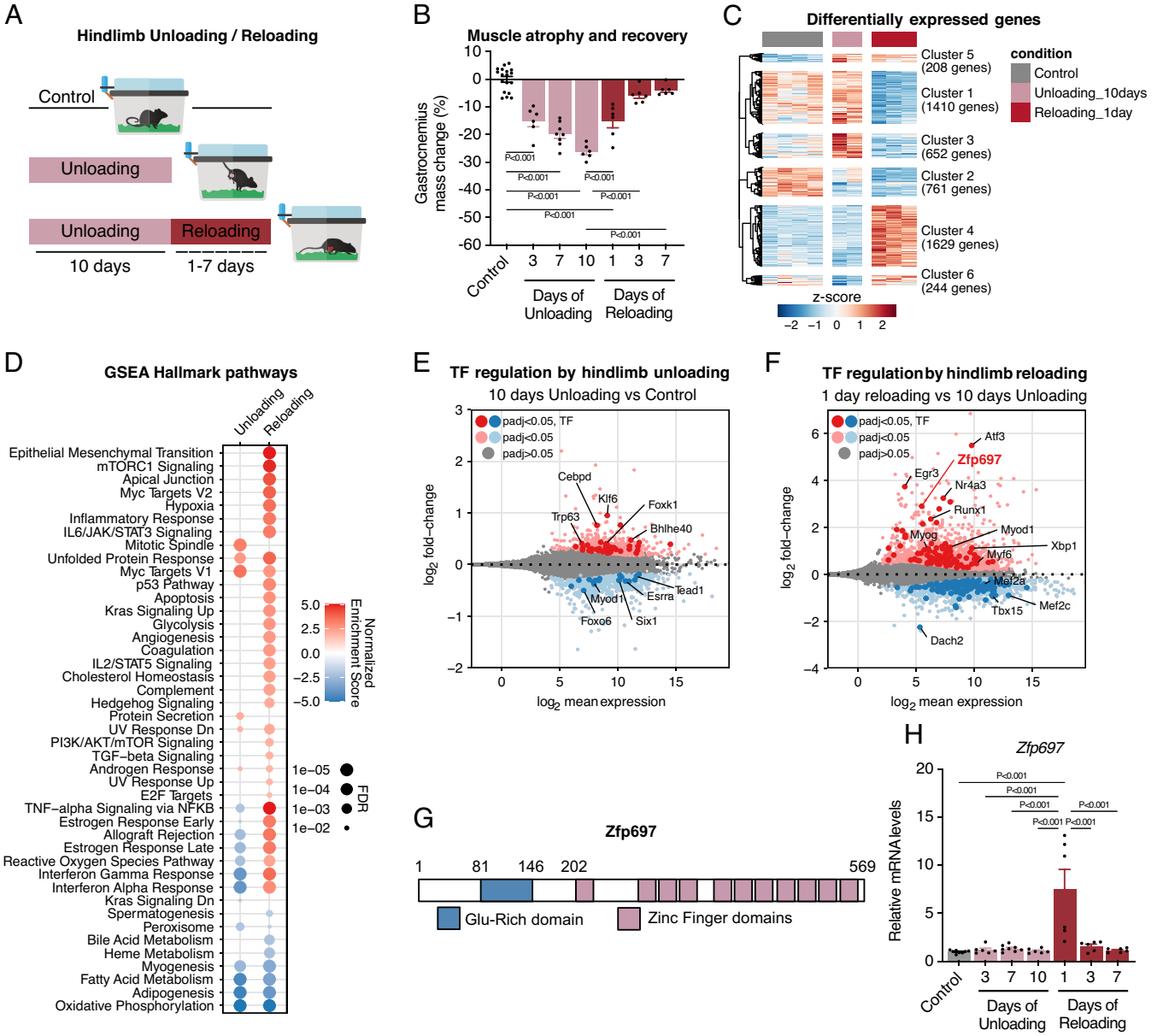


Fig. 1. Zfp697 expression increases during muscle recovery from atrophy. (*A*) Overview of the mouse hindlimb unloading and reloading protocol. (*B*) Change in mouse gastrocnemius mass (normalized by tibia length) during hindlimb unloading and reloading (n = 6 to 18). One-way ANOVA with Tukey's multiple comparisons test. (*C*) RNA-seq of mouse gastrocnemius muscle after 10 d of hindlimb unloading, 10 d of unloading followed by 1 d of reloading, and controls (n = 2 to 4 per condition). Heatmap highlights genes differentially expressed between unloading compared with control mice, and reloading compared with unloading. (*D*) GSEA for hallmark pathways in mouse gastrocnemius after hindlimb unloading and reloading. FDR, false discovery rate. (*E* and *F*) MA plots of gene expression levels in mouse gastrocnemius after 10 d of unloading compared with control, and 1 d of reloading compared with 10 d of unloading. Red dots indicate genes with significantly increased expression, while blue dots indicate genes with significantly decreased expression (*P*adj < 0.05). Known and putative transcriptional factors are highlighted. TF, transcription factor; *P*adj, adjusted *P*-value. (*G*) Schematic representation of the Zfp697 protein and its predicted glutamine-rich and zinc finger structural domains. The numbers shown refer to amino acid positions in the mouse Zfp697 protein. (*H*) Zfp697 gene expression in mouse gastrocnemius during hindlimb unloading and reloading (n = 6 to 8). One-way ANOVA with Tukey's multiple comparisons test. Data represent mean values and error bars represent SEM.

we performed global gene expression analysis by RNA-sequencing (RNA-seq) of gastrocnemius muscles. Muscles were collected from control mice, mice at 10 d of unloading-induced muscle atrophy (hindlimb unloading) and from mice returned to normal cage activity for 1 d (reloading) (Fig. 1*C*, *SI Appendix*, Fig. S1 *A* and *B*, and Dataset S1). Gene set enrichment analysis (GSEA) of "unloading vs. control" and "reloading vs. unloading", performed with hallmark gene sets (11), revealed in common between both groups a repression of oxidative metabolism and myogenesis-related pathways and an induction on unfolded protein response (Fig. 1*D* and Dataset S2). Among the pathways repressed with unloading but induced with reloading we found NF-kB and IFNα and γ signaling. Unique to the early reloading set were pathways related to epithelial–mesenchymal transition, mTORC signaling, hypoxia and angiogenesis, glycolysis, and TGF-beta signaling (Fig. 1*D*). To identify potential upstream regulators of genes involved in those different biological processes, we overlapped our RNA-seq data with a list of known and predicted transcription factors (TFs) (12). With this approach, we identified several well-known regulators of muscle stress response (Atf3, Xbp1) (13), metabolism (Nr4a3) (14), and regeneration (Runx1, Mef2c) (15) (Fig. 1 *E* and *F*). Among the transcripts increased during the reloading phase we found the previously uncharacterized Zfp697 (which is annotated in ref. 12 as a putative TF) (Fig. 1*F*). Since Zfps are a group of versatile proteins with diverse biological activities and mechanisms of action, that includes several TFs (16), we decided to investigate the role of Zfp697 in skeletal muscle. Zfp697 encodes a 569 amino acid protein with an N-terminal glutamine-rich domain, followed by eleven C2H2 zinc finger domains (Fig. 1*G*). qRT-PCR analysis of muscle samples from the unloading/reloading time course shown in Fig. 1 *A* and *B*, confirmed that although Zfp697 levels don't change during the unloading period, they increase 7.5-fold after 1 d of reloading, and quickly return to baseline at day 3 (Fig. 1*H*). In a similar fashion, ZNF697 was also increased in human skeletal muscle upon ambulatory reloading following limb unloading (*SI Appendix*, Fig. S1 *C* and *D*) (17).

Interestingly, analysis of muscle RNA-seq data from an unloading/reloading protocol using adult vs. old mice (18), revealed a similar reloading-induced increase in Zfp697 levels in adult mice, that was lost in the aged group (where it is already elevated in controls) (*SI Appendix*, Fig. S1*E*). Additional analysis of skeletal muscle RNA from different mouse models or interventions revealed that Zfp697 is also transiently elevated in response to β_2-adrenergic receptor (β_2-AR) agonism (Fig. 2*A*). Additional stimuli that elevated Zfp697 included intense exercise (Fig. 2B), muscle injury (Fig. 2C), and lipopolysaccharide administration (LPS, *SI Appendix*, Fig. S2*A*). In human skeletal muscle, ZNF697 expression was also transiently increased following aerobic, resistance, or high intensity interval training (Fig. 2 *D* and *E*). Interestingly, Zfp697 expression remained elevated in situations of unresolved muscle damage such as muscular dystrophy (Fig. 2*F*) (19, 20) or cancer-related cachexia (Fig. 2*G*) (21, 22). In agreement with the data shown in *SI Appendix*, Fig. S1*E*, we determined that Zfp697 expression in mouse muscle progressively increases with age (Fig. 2*H*) and is strongly increased in a model of denervation (*SI Appendix*, Fig. S2*B*). ZNF697 expression was also higher in muscle of type 2 diabetic patients, following exercise (*SI Appendix*, Fig. S2*C*) (23).

Zfp697 Mediates the IFNγ Response in Muscle Cells. To determine which cell types within the muscle tissue express Zfp697 we queried the publicly available single-cell RNA sequencing (scRNA-seq) resources MyoAtlas (24) and datasets for regenerating skeletal muscle stromal vascular fraction (i.e., mononuclear cells) (25). These analyses revealed that at baseline Zfp697 is expressed in mature fibers in both soleus and TA muscles (Fig. 2*I* and *SI Appendix*, Fig. S2*D*). Both muscles show Zfp697 expression in other cell types most notably in soleus fibroadipogenic progenitors (FAPs) and endothelial cells (Fig. 2*I*). Nonfiber expression can also be seen in mononuclear cells in regenerating muscle (Fig. 2*J*). To begin uncovering the biological role of Zfp697 we used recombinant adenovirus to increase or silence Zfp697 expression in mouse primary myotubes (vs. a GFP or scrambled shRNA control, respectively) (Fig. 3*A*). Initial analysis by qRT-PCR focused on some of the genes highlighted in the gastrocnemius reloading RNA-seq analysis (Fig. 1*D*), namely cytokines and chemokines. With this approach we determined that Zfp697 expression in myotubes positively correlated with the mRNA expression for the analyzed cytokines and chemokines, in both gain- and loss-of-function experiments (Fig. 3*B*). To better understand the overall effects of Zfp697 in myotubes, we performed RNA-seq under the gain-of-function experimental conditions (*SI Appendix*, Fig. S3*A* and Dataset S3). GSEA for hallmark pathways highlighted, among others, IFN response, JAK/STAT signaling, and inflammatory response (Fig. 3*C*, *SI Appendix*, Fig. S3*B*, and Dataset S4) which largely overlapped with pathways observed for the reloaded gastrocnemius muscle (Fig. 1*D*). In particular, the IFNγ response pathway (Fig. 3*C*) and its main target genes (Fig. 3*D*) were consistently highlighted. Moreover, GSEA for cellular component pathways suggested the induction of transcriptional programs related to ECM remodeling, vesicle trafficking, and secretory apparatus (*SI Appendix*, Fig. S3*B* and Dataset S4). Analysis of distant regulatory elements (DiRE) (26) predicted to mediate the observed gene expression patterns, revealed that genes induced by Zfp697 are also potentially regulated by the transcription factor families STAT and SMAD (*SI Appendix*, Fig. S3*C*). Interestingly, there are several evolutionarily conserved STAT binding sites within the proximal promoter for the Zfp697 gene (*SI Appendix*, Fig. S3*D*), which proved to be inducible in myotubes by IFNγ treatment but not by TNFα (*SI Appendix*, Fig. S3*E*). Together, these data and the fact that IFNγ has been implicated in muscle regeneration (27, 28), prompted us to investigate whether Zfp697 is part of the IFNγ signal transduction pathway. We next treated mouse primary myotubes with recombinant IFNγ after silencing Zfp697 expression (vs. a scrambled control shRNA). Although *Zfp697* transcription was only modestly induced by IFNγ treatment, it was required for the basal expression of several chemokines and known IFNγ target genes. Zfp697 also proved to be strikingly necessary for IFNγ response (Fig. 3 *E* and *F*). When comparing genes regulated by Zfp697 expression in primary myotubes with genes differentially expressed in the reloaded mouse gastrocnemius, we identified 535 shared genes with increased expression (*SI Appendix*, Fig. S3*F* and Dataset S5). These clustered around pathways of cell adhesion, immune cell recruitment, and cytokine-mediated cell–cell communication genes with commonly decreased expression highlighted metabolic pathways such as mitochondrial respiratory chain complex I assembly and aerobic respiration (*SI Appendix*, Fig. S3*G* and Dataset S5). Focusing this analysis specifically on IFNγ target genes, we observed a significant overlap between those increased by ectopic Zfp697 expression in myotubes and those increased during the early reloading stage (when Zfp697 itself is increased) (*SI Appendix*, Fig. S3*H*).

Zfp697 Is an RNA-Binding Protein that Targets lncRNAs and miRNAs. Since Zfp697 is mostly composed of zinc finger domains, we first thought it could function as a DNA binding TF. To test that possibility, we performed chromatin immunoprecipitation followed by sequencing (ChIP-seq) in mouse primary myotubes expressing Flag-Zfp697 or a GFP control. These experiments were performed under the same conditions as for the RNA-seq. We used a Flag-tagged version of Zfp697 since there were no available

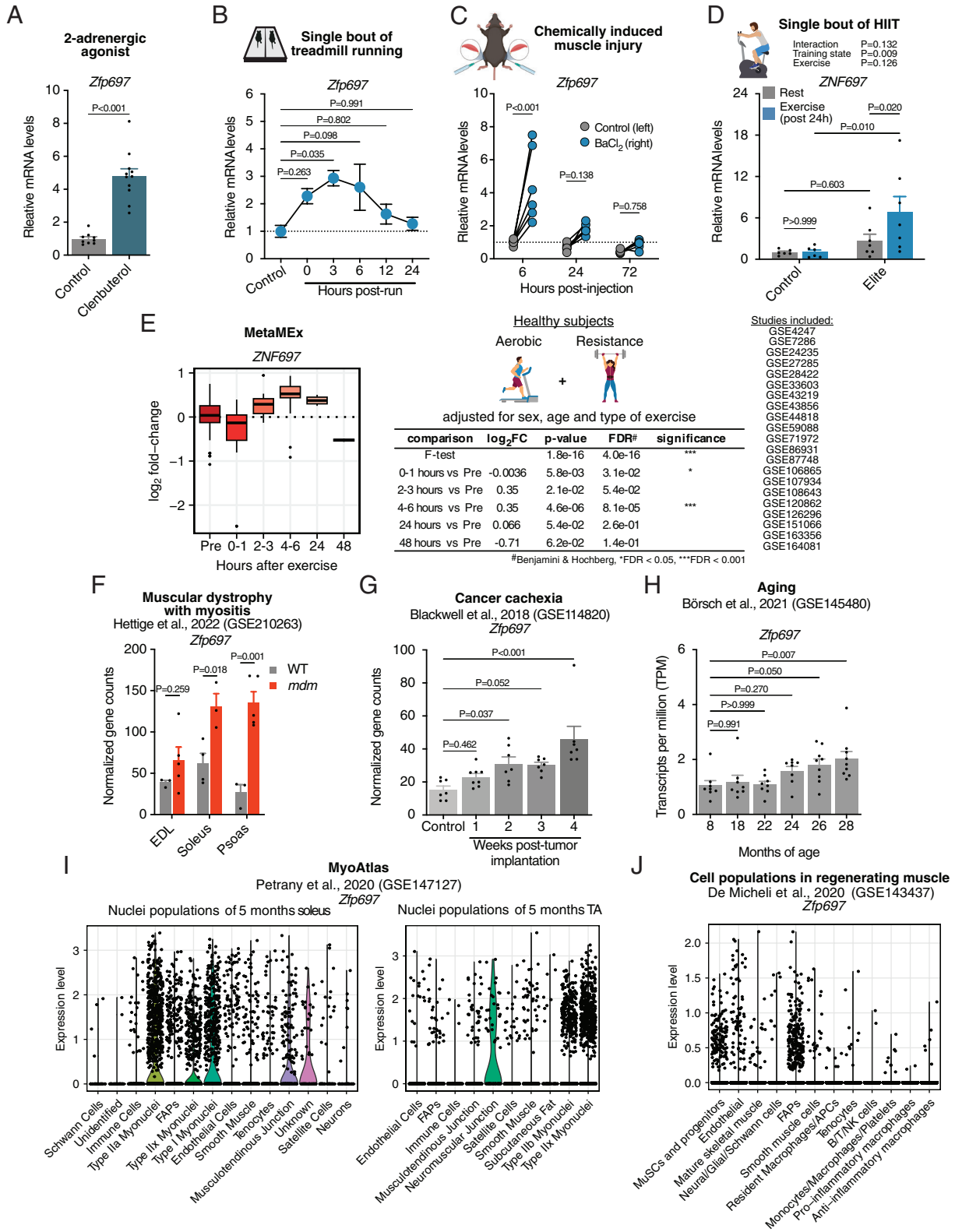


Fig. 2. Zfp697/ZNF697 expression is transiently elevated during recovery from injury. (*A*) Zfp697 gene expression in mouse gastrocnemius (gastroc) 16 h after clenbuterol injection (i.p. 2 mg/kg, n = 9 to 11). Two-tailed Student's *t* test. (*B*) Zfp697 gene expression in mouse quadriceps following a single bout of treadmill running at 0, 3, 6, 12, and 24 h, compared with the rest control (n = 4 to 6). One-way ANOVA with Dunnett's multiple comparisons test. (*C*) Zfp697 gene expression in mouse gastroc. after muscle injury induced by i.m. BaCl2 injection in the gastroc. of one leg (*Right*) and control solution in the same site of the contralateral leg (*Left*). Muscles were harvested 6, 24, and 72 h postinjection (n = 6 per time point). Two-way ANOVA with Šídák's multiple comparisons test. (*D*) ZNF697 gene expression in muscle biopsies taken before and 24 h after a single bout of high-intensity interval training in recreationally active subjects (Control) and elite athletes (Elite) (n = 6 to 7). Two-way ANOVA with Šídák's multiple comparisons test. (*E*) ZNF697 gene expression in human skeletal muscle after exercise (data from the MetaMEx database). (*F*) Zfp697 gene expression in skeletal muscles of mice with muscular dystrophy with myositis (mdm) compared with wild-type (WT) controls (dataset GSE210263). Two-tailed Student's *t* test. (*G*) Zfp697 gene expression in mouse gastroc. during cancer cachexia progression (dataset GSE114820). One-way ANOVA with Dunnett's multiple comparisons test. (*H*) Zfp697 gene expression in mouse gastroc. during aging (dataset GSE145480). One-way ANOVA with Dunnett's multiple comparisons test. (*I*) Zfp697 gene expression in nuclei isolated from soleus or tibialis anterior (TA) of 5-mo-old mice (dataset GSE147127). (*J*) Zfp697 gene expression in mononuclear cells isolated from regenerating muscle (dataset GSE143437).

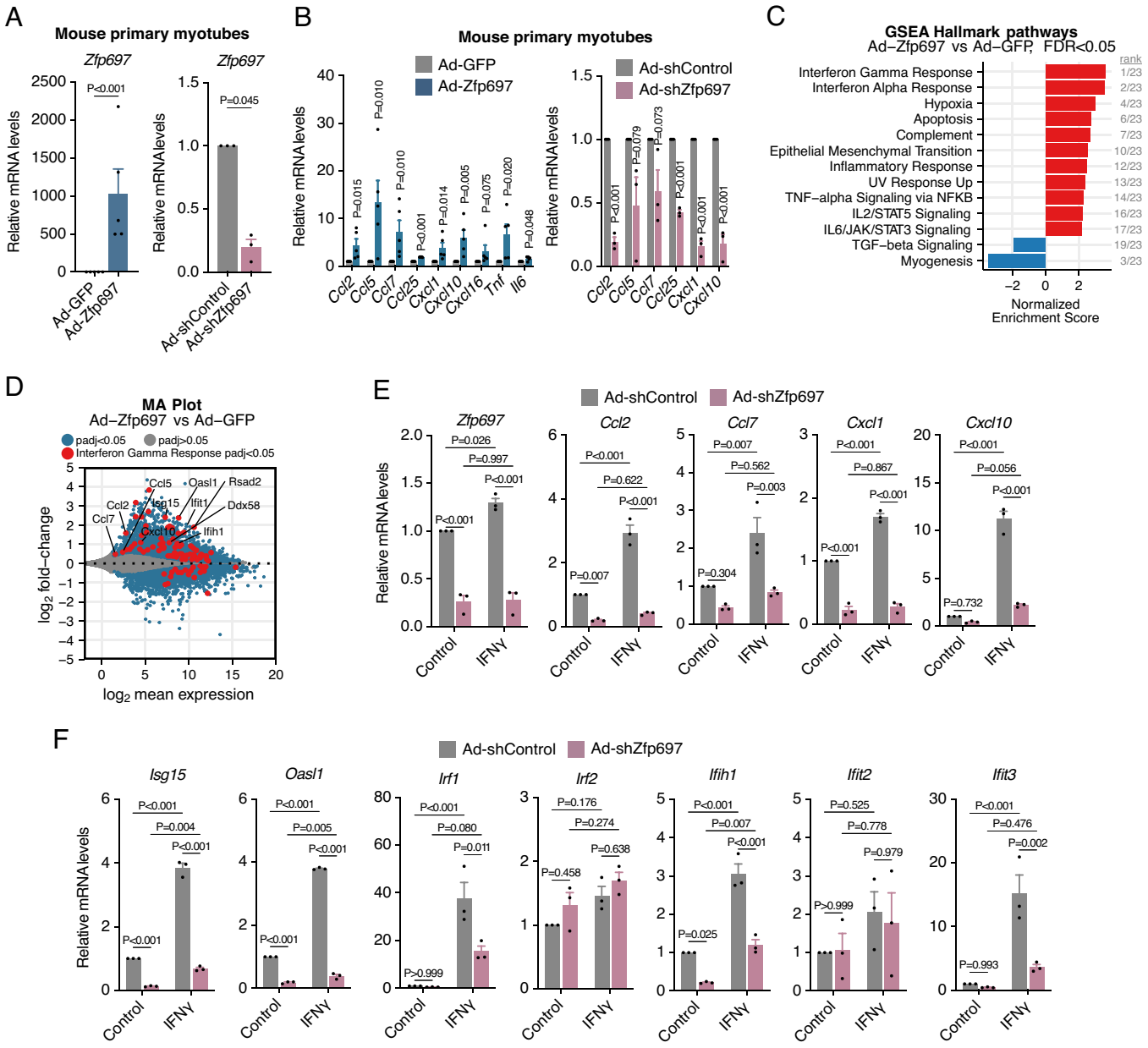


Fig. 3. Zfp697 is necessary for IFNg signal transduction in myotubes. (*A*) Zfp697 gene expression in mouse primary myotubes with Zfp697 gain- or loss-of-function. For gain-of-function experiments, fully differentiated myotubes were transduced with adenovirus expressing GFP alone (Ad-GFP) or together with Zfp697 (Ad-Zfp697; n = 5 independent experiments). For loss- of-function, cells were transduced with adenovirus expressing Zfp697-specific (Ad-shZfp697) or scrambled control shRNAs (Ad- shControl; n = 3 independent experiments). Two-tailed Student's paired t test vs. respective control. (*B*) Gene expression analysis of chemokines in mouse primary myotubes with Zfp697 gain- or loss-of-function. Two-tailed Student's paired *t* test vs. respective control. (*C*) GSEA for hallmark pathways in mouse primary myotubes overexpressing Zfp697. FDR, false discovery rate. (*D*) MA plot showing mean gene expression vs. log2 fold-change in mouse primary myotubes overexpressing Zfp697. Differentially expressed genes are shown in blue (*P*adj < 0.05). IFNγ response genes are highlighted in red. *P*adj, adjusted *P*-value. (*E* and *F*) Gene expression analysis of Zfp697, chemokines, and IFNγ response genes in mouse primary myotubes after Zfp697 loss-of-function and treated with IFNγ or control (20 ng/mL for 8 h; n = 3 independent experiments). Two-way ANOVA with Tukey's multiple comparisons test. Data represent mean values and error bars represent SEM.

antibodies that specifically recognize the endogenous protein, despite our own efforts to generate such a reagent. Surprisingly, the results from these experiments revealed very few chromatin regions associated with Flag-Zfp697 (*SI Appendix*, Fig. S4*A*). Although these data do not conclusively prove that Zfp697 does not bind DNA, they suggest that Zfp697 might not work primarily as a TF. In support of this notion, we observed that purified GST-Zfp697 interacted with RNA in a pull-down assay (*SI Appendix*, Fig. S5*A*). This interaction relied on the zinc finger domains since a truncated mutant lacking the zinc finger domains bound RNA to the same level as GST alone (*SI Appendix*, Fig. S5*A*). To further investigate the RNA-binding properties of Zfp697 and identify Zfp697-bound RNAs, we performed enhanced crosslinking and immunoprecipitation (eCLIP) using the same primary myotube experimental setup as for the RNA-seq and the ChIP-seq experiments but analyzed by eCLIP followed by high-throughput sequencing (eCLIP-seq, *SI Appendix*, Fig. S5*B* and *C*) (29). With this approach we identified 501 Zfp697-associated reproducible enriched windows, corresponding to 457 unique genes, that were significantly enriched compared to a size-matched control (FDR < 0.05, enrichment odds ratio [OR] > 8) (Dataset S6). Zfp697 binding sites were depleted in introns and enriched in CDS

and UTR, indicating that it primarily binds spliced transcripts (*SI Appendix*, Fig. S5*D*). Most binding targets were protein-coding genes (*SI Appendix*, Fig. S5*E*). Additionally, we observed that miRNA binding was strongly enriched (OR = 11.5) compared to the size-matched control (*SI Appendix*, Fig. S5*F*). When compared to eCLIP results from the ENCODE 3 dataset (n = 223 eCLIP experiments), Zfp697 binds more miRNAs than 97% of other datasets, barely outranked by the miRNA processing factors DROSHA and DGCR8 (*SI Appendix*, Fig. S5*G*). Zfp697's top two binding motifs, when compared against ENCODE 3, matched most closely with Gemin5 (*SI Appendix*, Fig. S5*H*). Gemin3 and Gemin4 both participate in Ago2–miRNA complexes (30, 31), and Gemin5 has been proposed to play a similar role (32). Furthermore, Zfp697's third-ranked binding motif matched most closely with the miRNA biogenesis factor DGCR8 (*SI Appendix*, Fig. S5 *H*, *Bottom* panel). These results provide further support for Zfp697's binding preference for miRNA.

Interestingly, one of the top hits among Zfp697 miRNA targets was miR-206-3p, which has been previously shown to promote skeletal muscle regeneration (*SI Appendix*, Fig. S5*I*) (33, 34). In line with that observation, we determined that myotubes overexpressing Zfp697 exhibit reduced abundance of the miR-206-5p passenger strand, suggesting Zfp697 promotes the usage of miR-206-3p as the mature strand (*SI Appendix*, Fig. S5*J*) (35). In agreement, analysis of the mRNA abundance for miR-206-3p targets previously reported to be downstream of its regenerative effects in muscle (33), showed the expected reduction in Zfp697-expressing myotubes, although not for all genes (*SI Appendix*, Fig. S5*K*).

Myofiber-Specific Zfp697 Knockout Compromises Muscle Recovery from Atrophy and Injury. To test the effects of Zfp697 expression in vivo, we used adenovirus-mediated gene delivery by intramuscular injection in SCID mice (vs. a GFP control in the contralateral limb; *SI Appendix*, Fig. S6*A*). This resulted in a mild but sustained overexpression of Zfp697 until 7 d postinjection (*SI Appendix*, Fig. S6*B*). Targeted qRT-PCR analysis of some of the pathways highlighted by the previous RNA-seq datasets, revealed that muscles transduced with the Zfp697-encoding adenovirus (vs. the GFP transduced contralateral limb) had higher expression levels of several chemokines and their receptors (*SI Appendix*, Fig. S6 *C* and *D*), genes related to IFNγ signaling (*SI Appendix*, Fig. S6*E*), immune cell markers (*SI Appendix*, Fig. S6*F*), and ECM remodeling genes (*SI Appendix*, Fig. S6*G*). In line with these gene expression patterns, we could detect signs of tissue fibrosis by immunohistochemical analysis of the transduced muscle (*SI Appendix*, Fig. S7 *A* and *B*). Importantly, we also determined that Zfp697/ZNF697 expression is robustly increased in situations of disease with a strong unresolved inflammation and fibrosis component. These included mouse kidney injury and different mouse models of heart failure and dysfunction (*SI Appendix*, Fig. S7 *C* and *D*).

To evaluate the consequences of loss of Zfp697 function in muscle, considering the Zfp697 expression pattern, and the data obtained with cultured myotubes, we generated a myofiber-specific Zfp697 knockout mouse (Zfp697 mKO). This was achieved by creating a mouse line carrying loxP sites flanking the coding sequence within exon3 of Zfp697 (which encodes 86% of the protein, including all zinc finger domains) (Fig. 4*A*), which was crossed with the Mef2c enhancer/myogenin promoter-Cre line (36) (Fig. 4*A* and *SI Appendix*, Fig. S8*A*). As expected, Zfp697 mKOs showed reduced but not absent Zfp697 expression in muscle tissues (reflecting Zfp697 expression in other cell types), and no changes in any other analyzed tissue (*SI Appendix*, Fig. S8*B*). At baseline, no differences were seen between genotypes in terms of body weight, muscle tissue mass, exercise performance, or grip strength (*SI Appendix*, Fig. S8 *C–F*). Zfp697 mKO mice and floxed littermate controls were then subjected to the unloading/reloading protocol. Each genotype was divided into control (no unloading or reloading), 10 d unloading, and two additional groups that were unloaded for 10 d followed by 1 or 3 d of reloading (Fig. 4*B*). In line with our previous results, Zfp697 expression was elevated in muscles from floxed controls during reloading (Fig. 4*C*). This regulation was completely blunted in Zfp697 mKO mice (Fig. 4*C*), further indicating that, in this context, that response comes mostly from the muscle fibers. Analysis of total body mass and composition during the experimental protocol revealed that Zfp697 mKO mice lost total, lean, and fat mass to a similar extent as floxed littermates, during the unloading phase (*SI Appendix*, Fig. S8*G*). In line with this, changes in muscle mass during the unloading phase were generally comparable between Zfp697 mKOs and floxed littermates except for the TA, that showed reduced wasting in Zfp697 mKO mice (Fig. 4*D*). Conversely, upon reloading Zfp697 mKOs showed reduced recovery of muscle mass in both gastrocnemius and TA muscle, with no significant differences observed in the soleus (Fig. 4*E*). In line with these observations, Zfp697 mKO mice had delayed recovery of lean mass. This was shown by a significant reduction in lean mass 1 d after reloading, compared to flox littermates (*SI Appendix*, Fig. S8*G*). The deficit in recovery observed in Zfp697 mKO mice was further evidenced by reduced extensor digitorum longus (EDL) and soleus absolute and specific force 3 d after reloading. This was especially clear at higher stimulation frequencies, as evident by significant interaction between genotype and stimulation frequency (*SI Appendix*, Fig. S8 *H* and *I*). Notably, there were no significant differences in fatigability and recovery (*SI Appendix*, Fig. S8 *H* and *I*). To further evaluate the implications of myofiber Zfp697 ablation in the functional recovery from muscle injury, we used two further models. First, we evaluated the kinetics of muscle force-production recovery after a single bout of downhill running, commonly used approach to elicit exercise-induced muscle damage due to the extensive use of eccentric contractions. Under these conditions, floxed control mice displayed the expected decline in grip strength over the first 48 h, followed by a swift recovery to normal values (Fig. 4*F*). In sharp contrast, Zfp697 mKO did not recover any grip strength by the latest time point analyzed (96 h) (Fig. 4*F*). In addition, we performed intramuscular cardiotoxin (CTX) injections, a myotoxic agent, and monitored functional decline and recovery using gait analysis (Fig. 4*G*). This assessment revealed a more pronounced decline in various gait parameters in Zfp697 mKO mice, including stride length, stance, and propulsion (Fig. 4*G*). Together, these data from various models of muscle injury and recovery indicate that Zfp697 ablation in myofibers compromises skeletal muscle regeneration and functional recovery.

Reloaded Zfp697 mKO Muscle Fails to Activate a Regenerative Gene Program. To complement the functional analysis of the unloading/reloading experiments we performed RNA-seq of the gastrocnemius muscles of the different groups of Zfp697 mKO and controls. This analysis was designed to account for the interaction effect between conditions (control, unloading, and reloading) and genotypes. When comparing Zfp697 mKOs and controls for changes in gene expression upon unloading, we saw no differences between genotypes (Fig. 5 *A* and *B* and *SI Appendix*, Fig. S9*A*). However, we observed a profound effect on the regenerative/remodeling response to reloading (Fig. 5 *A–C*). Among the differentially expressed genes, most increased in controls upon reloading but failed to be induced in Zfp697 mKO

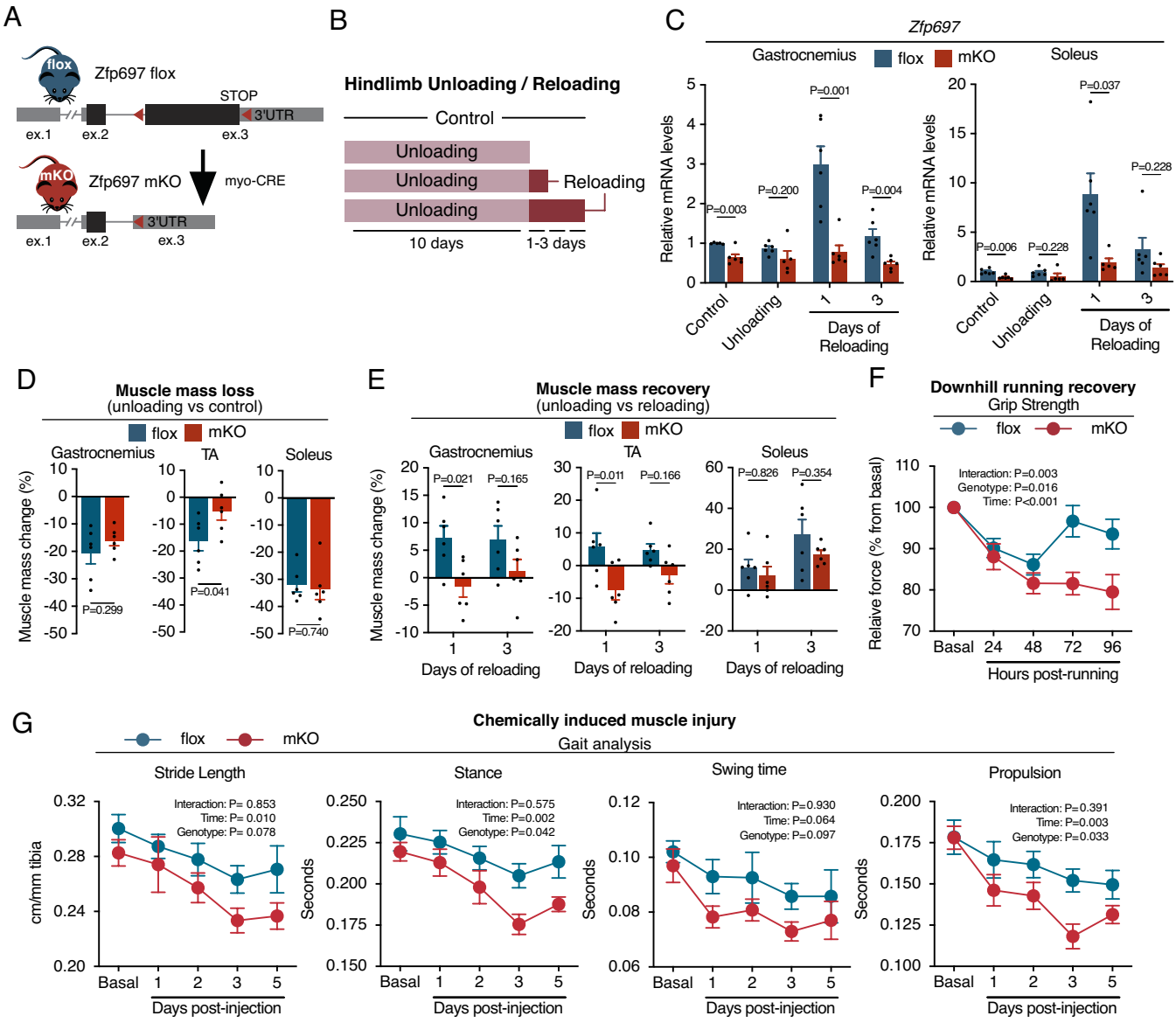


Fig. 4. Skeletal muscle-specific Zfp697 knockout blunts recovery from injury. (*A*) Schematic representation of the strategy adopted to generate skeletal-muscle specific Zfp697 knockout mice (Zfp697-mKO) and flox controls. Red arrows indicate loxP sites location. (*B*) Experimental approach for hindlimb unloading and reloading of Zfp697-mKO and flox littermates. (*C*) Zfp697 gene expression in the gastrocnemius (*Left* panel) and soleus (*Right* panel) of Zfp697-mKO and flox littermates following hindlimb unloading and reloading. Two-tailed Student's *t* test compared with time-matched flox controls. (*D*) Muscle mass change after 10 d of hindlimb unloading comparing Zfp697-mKO and flox littermates with preunloading genotype-matched controls (n = 6). Two-tailed Student's *t* test. (*E*) Muscle mass change after 1 or 3 d of hindlimb reloading comparing Zfp697-mKO and flox littermates with genotype-matched 10 d of unloaded mice (n = 6). Two-way ANOVA with Šídák's multiple comparisons test. (*F*) Change in body-weight-normalized grip strength following a single bout of strenuous downhill running in Zfp697-mKO mice and flox littermates (n = 10). Repeated measures two-way ANOVA with Šídák's multiple comparisons test. (*G*) Gait analysis of Zfp697-mKO mice and floxed littermates (flox, n = 5; mKO, n = 4) at baseline and following chemically induced muscle injury. Cardiotoxin was intramuscularly injected in the gastrocnemius and TA muscles of one leg (*Right*) and control solution in the same site of contralateral leg (*Left*). Repeated measures two-way ANOVA. Data represent mean values and error bars represent SEM.

muscle (Fig. 5*B* and Dataset S7), with a smaller subset changing in the opposite direction. These genes were associated with stress response, protein synthesis, IFNγ, and inflammatory responses (Fig. 5 *C* and *D* and Dataset S8), indicating failure of Zfp697 mKO muscle to activate a regenerative response to injury. Muscle regeneration is a complex process that relies on the coordinated action of multiple cell types, many of which are recruited and/or proliferate at the regenerating site. To better understand how Zfp697 ablation in myofibers affected other resident and recruited cell types during reloading-induced regeneration, we deconvoluted our RNA-seq data using CIBERSORTx (37) and a previously published single-cell RNA-seq data obtained from mouse regenerating muscle (25). This analysis provided an estimation of the relative abundance of different cell types using gene signatures from a mixed cell population RNA-seq dataset. The results shown in Fig. 5*E* and *SI Appendix*, Fig. S9*B* showed that after 3 d of reloading, the fraction of FAPs and muscle stem cells (satellite cells, MuSCs) had expanded in the floxed control muscles, but not in the Zfp697 mKOs. Indeed, immunohistochemistry quantification of Pax7-positive cells further revealed a reduction in the number of satellite cells in reloaded mKO muscle, compared to reload flox muscle (*SI Appendix*, Fig. S9*C*). In line with these data, we observed an increase in the number of proliferative KI67-positive cells in control muscles, which was significantly reduced in Zfp697 mKOs (Fig. 5*E*). The total area occupied by PDGFRα-positive

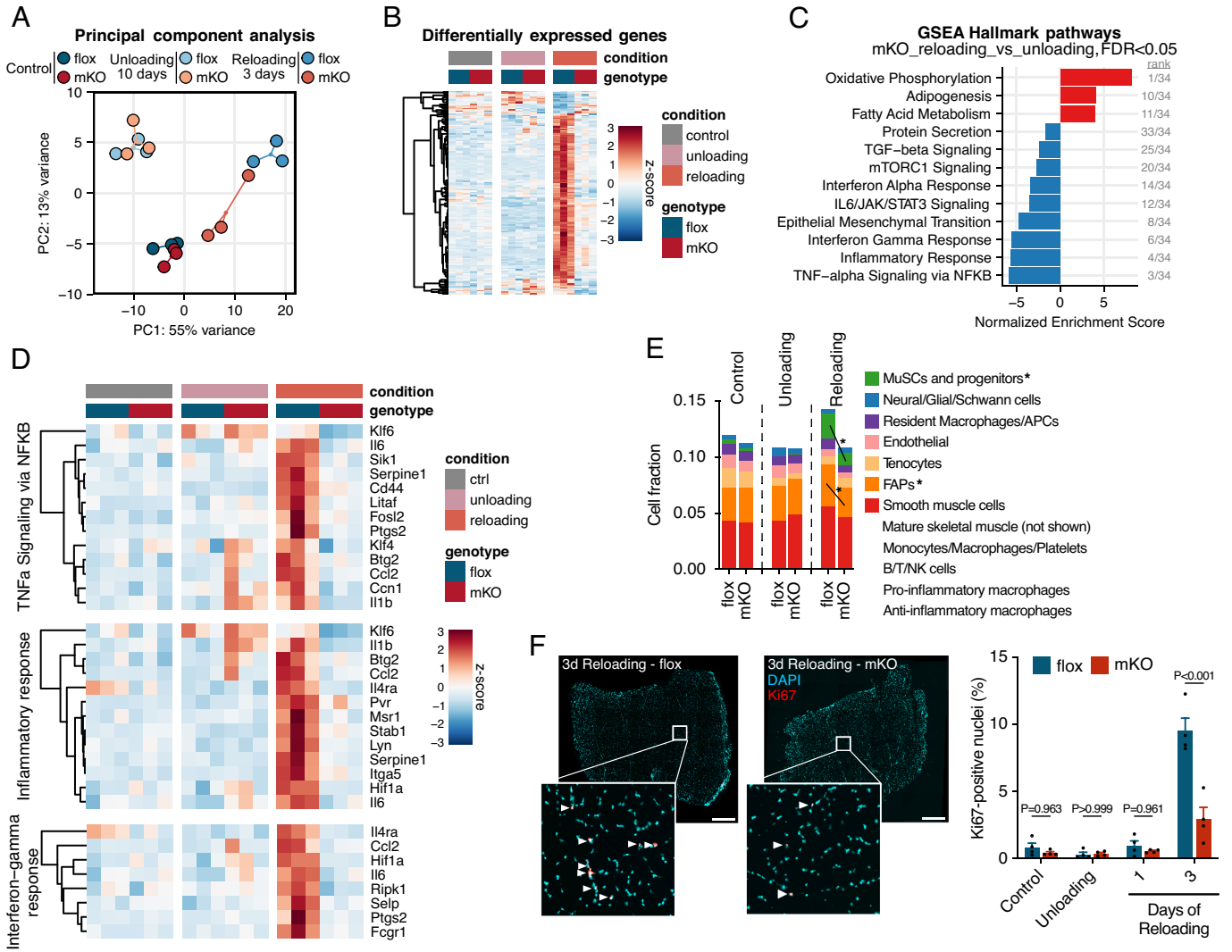


Fig. 5. Zfp697 mKOs fail to activate gene expression necessary for regeneration. (*A*) Principal component analysis for RNA-seq performed in the gastrocnemius muscle of control Zfp697 flox and mKO, after 10 d of hindlimb unloading and 3 d of reloading (n = 3 per condition and genotype). (*B*) Heatmap of differentially expressed genes for the interaction effect between conditions and genotypes. (*C*) GSEA for hallmark pathways accounting for the interaction effect between conditions (control, unloading, and reloading) and genotypes (mKO and flox). FDR, false discovery rate. (*D*) Heatmap of genes belonging to inflammatory and interferon-gamma response pathways. (*E*) Fraction of muscle-resident cell populations identified by digital cytometry (CIBERSORTx) applied to bulk muscle RNA-seq data from control, hindlimb unloaded, and reloaded Zfp697 flox and mKO mice (n = 3 per condition and genotype). Two-way ANOVA with Šídák's multiple comparisons test. *$P < 0.05$ between indicated cell types. (*F*) Immunostaining for proliferating cells using KI67 in gastrocnemius muscles of Zfp697 flox and mKO and respective quantification (n = 4 per condition and genotype). Two-way ANOVA with Šídák's multiple comparisons test. *P*-values represent comparison with time-matched flox controls. (Scale bar, 500 μm.)

cells was however similar between genotypes across all stages (*SI Appendix*, Fig. S9*D*), suggesting that the transcriptional changes observed might be reflective of activation state rather than abundance. Overall, these data indicate that Zfp697 mKO mice failed to activate a regenerative transcriptional program in myofibers during the early stages of recovery from hindlimb unloading, which affected not only the myofibers themselves but also other resident and infiltrating cells.

Together, our data identify Zfp697 as an RBP that preferentially binds ncRNAs, in particular miRNAs, and controls muscle remodeling. In skeletal muscle, Zfp697 is downstream of IFNγ signaling and is necessary for the activation of many of its target genes. Loss of Zfp697 action results in compromised muscle regeneration, whereas sustained expression leads to tissue inflammation and fibrosis. Collectively, these findings uncover Zfp697 as a promising therapeutic candidate for diseases where unresolved tissue inflammation and ECM remodeling are central disease components.

Discussion

Progressive loss of skeletal muscle mass and function is a major clinical feature of several neuromuscular diseases. It is also commonly observed in patients with chronic diseases such as cancer and is a major contributor to frailty and loss of independence during aging. To better understand the molecular determinants of skeletal muscle atrophy and subsequent recovery, we used a mouse model of hindlimb hypokinesia/hypodynamia (38). This model is often used to assess the effects of, for example, long-term bedrest and space flight on muscle mass and function. This protocol, commonly referred to as hindlimb unloading/reloading, offers the advantage of monitoring phenotypic and molecular changes during the progression of muscle atrophy and compensatory hypertrophy/regeneration over time, using the same animals. Among prominent transcriptional regulators of myogenesis, inflammation, and stress response (e.g., Myog, MyoD1, Atf3, RunX1), all of which are important components for the regenerative response to damage,

we found Zfp697 as a previously uncharacterized transcript which is elevated during the early stages of hindlimb reloading. We further verified that mouse Zfp697 expression is transiently induced in multiple settings associated with myofiber damage and remodeling, such as chemically induced injury and intense physical exercise. By analyzing a vast array of published transcriptomics data, we observed a similar expression profile in human skeletal muscle. In line with its expression profile, Zfp697 expression is enriched in a regenerative myonuclear population recently identified in dystrophic mouse muscle (RegMyon) (39) and a yet uncharacterized Ampd3$^+$ (AMP deaminase 3) myonuclear population in aged mouse muscle (*SI Appendix*, Fig. S2*D*), hypothesized to constitute dysfunctional denervated fibers (24). In support of this notion, Zfp697 expression is highly induced in denervated mouse muscle (*SI Appendix*, Fig. S2*B*). All these data position Zfp697 at the center of the regenerative response in several physiological and pathophysiological contexts.

Muscle regeneration is a complex process that relies on the coordinated action of multiple resident and infiltrating cells. In this context, inflammatory signals have emerged as important regenerative signals. They have been implicated not only in the regulation of immune cell behavior but also satellite cell proliferation, myogenesis, FAP activation, ECM remodeling, and myofiber metabolic adaptations (3, 40). Here, we show that activation of Zfp697 in the muscle fiber is upstream of that cascade of events. Zfp697 activates a broad inflammatory gene program in cultured myotubes and intact mouse muscle, including a large array of chemokines implicated in immune cell recruitment and muscle regeneration (40–44). The transcriptional profile brought about by ectopic Zfp697 expression was particularly enriched for the IFNα and γ pathways. Conversely, IFNα and γ response pathways were among the top pathways associated with genes dysregulated in Zf697 mKO mice upon hindlimb reloading. IFNγ signaling is activated in the early stages of skeletal muscle regeneration (which is further reinforced by our transcriptomics data on reloaded muscle) and endogenous IFNγ is necessary for efficient skeletal muscle regeneration (27, 45). Moreover, the age-related decline in tissue macrophage responses to IFNγ contributes to poor regenerative capacity, by impairing satellite cell proliferation and differentiation (28). Strikingly, Zfp697 knockdown in myotubes reduced not only the basal expression of interferon-stimulated genes, but also strongly blunted the response to exogenous IFNγ. This indicates that Zfp697 is an important mediator of IFN signaling in skeletal muscle cells. Interestingly, genetic variants in the ZNF697 genomic locus have been associated with the response of multiple sclerosis patients to IFNβ treatment (46), indicating that the role of Zfp/ZNF697 in IFN signaling is conserved in humans and in multiple cell types.

In line with the transient nature of Zfp697 activation in regenerating skeletal muscle, myofiber-specific in vivo loss-of-Zfp697 function (Zfp697 mKO mice), has negligible effects on animals kept under control conditions, or even when they are subjected to hindlimb unloading. Likewise, the transcriptional profile of Zfp697 mKO at rest or following hindlimb unloading was indistinguishable from that of flox littermate controls. This is somewhat surprising (at least to this extent) and it does not recapitulate the strong effect of Zfp697 loss-of-function on the expression of chemokines and interferon-stimulated genes in cultured myotubes. It is possible that the higher expression of these transcripts in other cell types masks potential differences in gene expression in myofibers. It is also possible that the effects of Zfp697 are potentiated in regenerating fibers, a phenotype that may be better reflected by differentiated myotubes than by unchallenged mature fibers. In sharp contrast, the regenerative response to damage is severely compromised in Zfp697 mKO mice. Using three different muscle injury-recovery paradigms (unloading/reloading, downhill running, and cardiotoxin) and complementary methods to monitor recovery over time, we were able to determine that myofiber Zfp697 is essential for skeletal muscle repair and functional recovery. Following injury, Zfp697 mKO mice display deficient recovery of muscle mass, myofiber contractile force, grip strength, and normal gait parameters. At the molecular level, this was accompanied by deficient activation of a regenerative gene program associated with inflammation, ECM remodeling, angiogenesis, and cell proliferation. Furthermore, Zfp697 mKOs show reduced satellite cell and fibro-adipogenic precursor activation upon hindlimb reloading, two cellular processes that are essential for efficient muscle regeneration (4, 47, 48).

Whereas transient activation of a regenerative response conducive to immune cell recruitment and ECM remodeling is critical for efficient repair and functional recovery, persistent activation of these pathways can lead to morphologic and metabolic abnormalities, overt fiber damage, and fibrosis. This is a hallmark of neuromuscular diseases, such as dermatomyositis and muscular dystrophy, and a common feature of cancer cachexia, metabolic diseases, and aging (49, 50). We found that the levels of Zfp697/ZNF697 are elevated in mouse and human muscle in disease situations characterized by unresolved inflammation, and chronic tissue remodeling, such as muscular dystrophy and cancer cachexia. This dichotomy between transient physiological activation and chronic pathological elevation is not uncommon, nor is the challenge to discern between a causative detrimental process and an attempt at rescue. In our study, ectopic Zfp697 expression in skeletal muscle over a period of 7 d led to increased collagen deposition and heightened expression of markers of inflammation and ECM remodeling, suggesting that chronically elevated Zfp697 may contribute to skeletal muscle dysfunction. As the pattern of Zfp697 expression is not restricted to skeletal muscle, it remains to be established to what extent it might contribute to the pathophysiology of different diseases.

ZFPs represent an abundant group of proteins, with diverse biological activities and mechanisms of action. ZFPs can interact with DNA, RNA, and other proteins and have as diverse cellular functions as regulation of transcription, DNA repair, signal transduction, protein degradation, among others (16). In skeletal muscle, ZFPs are known to regulate myoblast differentiation (i.e., KLF5) (51) and fusion (i.e., KLF2,4) (52), protein turnover and muscle mass (i.e., Murf1, LMCD1) (53, 54), metabolism and exercise adaptation (i.e., YY1, KLF15) (55, 56), among many other processes. Zfp697 contains eleven C2H2 zinc fingers, spanning most of the protein, which led us to test whether they could mediate DNA binding. Although our data suggest that in muscle Zfp697 is not primarily a DNA-binding TF, we cannot preclude that it may have that or other activities in a cell-type or context-specific manner. However, here we show that Zfp697 is a novel RBP that preferentially binds processed mRNAs and miRNAs. Indeed, Zfp697 scored very high in its specificity for miRNA binding, even when compared with the Microprocessor complex components, DROSHA and DGCR8 (57). Of particular interest, the top hit of the Zfp697 miRNA list was miR-206, one of the myomiRs, a set of conserved skeletal-muscle enriched miRNAs. Among these, miR-206 and miR-133b are processed from the pre-miRNA Lincmd1 (58). Notably, miR-206 has been previously shown to promote skeletal muscle regeneration and to delay both features of pathology in mouse models of Duchenne muscular dystrophy (DMD) and amyotrophic lateral sclerosis (ALS) in mice (33, 34). Concordant with the idea of physiologically transient vs. pathologically chronic elevation in the expression of regulators

of tissue regeneration, miR-206 has been found to be increased in circulation in ALS, muscular dystrophies, and Alzheimer's disease patients (among others), and even suggested as a disease progression biomarker (59). Of note, our eCLIP data also indicate an enrichment in repetitive sequences present in Zfp697-interacting RNAs. Although commonly filtered out during analysis due to the inability of mapping these sequences to unique identifiers, they often represent retrotransposable elements (60). When actively expressed (e.g., during cellular stress) the resulting dsRNAs are potent activators of interferon responses (61) and have been implicated in limb regeneration (62), autoimmunity (63), and immune cell infiltration in tumors (64).

Our study identifies Zfp697 as a novel RBP with a prominent role in skeletal muscle inflammation and regeneration. It is important to note that Zfp697 is not skeletal-muscle-specific and that the molecular and cellular processes that it regulates and important in multiple tissues and in various physiological and pathophysiological contexts. Indeed, a search of publicly available gene expression datasets indicates that Zfp697/ZNF697 expression is dysregulated in situations of unresolved inflammation and fibrosis, such as kidney and heart disease (*SI Appendix*, Fig. S5 *C* and *D*). The biological activities, expression patterns, signal transduction, and mechanisms of action we describe here indicate that Zfp697 can operate in diverse cell types and may be a valuable therapeutic target to improve tissue regeneration and modulate tissue inflammation.

Materials and Methods

All reagents and mouse models used in this study are commercially available or can be obtained by contacting the lead author. Experimental protocols as well as the details of experimental instruments are described in *SI Appendix*. All animal experiments were approved by the regional animal ethics committee of Northern Stockholm, Sweden. Methods included primary cell culture, eCLIP, ChIP, mouse hindlimb unloading/reloading, and evaluation of muscle function in vivo and ex vivo. The floxed Zfp697 mouse model was generated CRISPR/Cas9-mediated homology-directed repair, to include loxP sites in the intronic region upstream of exon 3 and within the 3′UTR region of exon 3.

Data, Materials, and Software Availability. Previously published data were used for this work (17–19, 22–25, 65–69). RNA Sequencing (GSE237099, GSE273092, and GSE273093) and https://github.com/ruaslab ChIP sequencing (GSE273094) data herein generated have been deposited in GEO (70–73). All other data are included in the manuscript and/or supporting information.

ACKNOWLEDGMENTS. We thank the Science for Life Laboratory, National Genomics Infrastructure, and Uppmax (Sweden). This work was supported by grants from The Swedish Research Council (2016-00785, 2019-01282, 2022-01650, and 80358701-03), The Novo Nordisk Foundation (NNF16OC0020804 and NNF22OC0075245), the NIH (HG009889, HG004569, HG011864, and CA273432), the Gösta Fraenckel Foundation for Medical Research, AFM-Tèlèthon, the European Association for the Study of Diabetes, the Åke Wibergs Foundation, the Olle Engqvist Foundation (207-0479). G.W.Y. is supported as an Allen Distinguished Investigator, a Paul G. Allen Frontier Group advised grant to the Paul G. Allen Family Foundation. P.G. received a Senior Research Fellowship (1117835) and an Investigator Grant (2017070) from the National Health and Medical Research Council of Australia. The Research Council of Lithuania (S-MIP-19-54) supported S.K. J.C.C. and I.C. were supported by a postdoctoral fellowship from SSMF and P.R.J. by the Wenner-Gren Foundations. M.L.G. was awarded an NSF Graduate Research Fellowship (DGE-2038238), a Myotonic Dystrophy Foundation Doctoral Research Fellowship, and an Association for Women in Science Scholarship. S.D. received a postdoctoral fellowship from the Swiss NSF. Q.L. was awarded an American Heart Association Predoctoral Fellowship.

Author affiliations: [a]Molecular and Cellular Exercise Physiology, Department of Physiology and Pharmacology, Biomedicum, Karolinska Institutet, Stockholm SE-171 77, Sweden; [b]Department of Cellular and Molecular Medicine, University of California, San Diego, La Jolla, CA 92093; [c]Sanford Stem Cell Institute Innovation Center and Stem Cell Program, University of California San Diego, La Jolla, CA 92093; [d]Center for RNA Technologies and Therapeutics, University of California San Diego, La Jolla, CA 92093; [e]Nanomedicine and Spatial Biology, Department of Physiology and Pharmacology, Biomedicum, Karolinska, Stockholm SE-171 77, Sweden; [f]Department of Cell and Molecular Biology, Biomedicum, Karolinska Institutet, Stockholm SE-171 77, Sweden; [g]Molecular Muscle Physiology and Pathophysiology, Department of Physiology and Pharmacology, Biomedicum, Karolinska Institutet, Stockholm SE-171 77, Sweden; [h]Department of Chemistry and Biochemistry, University of California San Diego, La Jolla, CA 92093; [i]Science for Life Laboratory, Department of Gene Technology, School of Engineering Sciences in Biotechnology, Chemistry and Health, KTH Royal Institute of Technology, Stockholm SE-100 44, Sweden; [j]Centre for Muscle Research, Department of Anatomy and Physiology, School of Biomedical Sciences, The University of Melbourne, Parkville, VIC 3010, Australia; [k]Muscle Physiology, Department of Physiology and Pharmacology, Biomedicum, Karolinska Institutet, Stockholm SE-171 77, Sweden; [l]Institute of Sports Science and Innovations, Lithuanian Sports University, Kaunas 44221, Lithuania; and [m]Department of Pharmacology and Stanley & Judith Frankel Institute for Heart & Brain Health, University of Michigan Medical School, Ann Arbor, MI 48109

Author contributions: J.C.C., P.R.J., M.L.G., I.C., S.D., S.M.P., K.D.D., Z.L., Q.L., H.W., T.V., M.B., S.K., J.T.L., G.W.Y., and J.L.R. designed research; J.C.C., P.R.J., M.L.G., I.C., S.D., S.M.P., J.M.D., K.D.D., Z.L., Q.L., P.G., T.V., M.B., and S.K. performed research; P.G. contributed new reagents/analytic tools; J.C.C., P.R.J., M.L.G., I.C., S.D., S.M.P., J.M.D., K.D.D., Z.L., Q.L., D.E., O.E., H.W., T.V., M.B., S.K., J.T.L., A.I.T., G.W.Y., and J.L.R. analyzed data; A.I.T. supervision; and J.C.C., P.R.J., and J.L.R. wrote the paper.

1. L. S. Chow *et al.*, Exerkines in health, resilience and disease. *Nat. Rev. Endocrinol.* **18**, 273–289 (2022).
2. R. Furrer, J. A. Hawley, C. Handschin, The molecular athlete: Exercise physiology from mechanisms to medals. *Physiol. Rev.* **103**, 1693–1787 (2023), 10.1152/physrev.00017.2022.
3. S. M. Hindi, D. P. Millay, All for one and one for all: Regenerating skeletal muscle. *Cold Spring Harb. Perspect. Biol.* **14**, a040824 (2022).
4. A. W. B. Joe *et al.*, Muscle injury activates resident fibro/adipogenic progenitors that facilitate myogenesis. *Nat. Cell Biol.* **12**, 153–163 (2010).
5. C. Bernard, A. Zavoriti, Q. Pucelle, B. Chazaud, J. Gondin, Role of macrophages during skeletal muscle regeneration and hypertrophy-Implications for immunomodulatory strategies. *Physiol. Rep.* **10**, e15480 (2022).
6. D. Burzyn *et al.*, A special population of regulatory T cells potentiates muscle repair. *Cell* **155**, 1282–1295 (2013).
7. M. V. Plikus *et al.*, Fibroblasts: Origins, definitions, and functions in health and disease. *Cell* **184**, 3852–3872 (2021).
8. L. R. Smith, E. R. Barton, Regulation of fibrosis in muscular dystrophy. *Matrix Biol.* **68–69**, 602–615 (2018).
9. E. R. Morey, Spaceflight and bone turnover: Correlation with a new rat model of weightlessness. *BioScience* **29**, 168–172 (1979).
10. J. L. Ruas *et al.*, A PGC-1α isoform induced by resistance training regulates skeletal muscle hypertrophy. *Cell* **151**, 1319–1331 (2012).
11. A. Liberzon *et al.*, The molecular signatures database hallmark gene set collection. *Cells* **1**, 417–425 (2015).
12. S. A. Lambert *et al.*, The human transcription factors. *Cell* **172**, 650–665 (2018).
13. S. He *et al.*, IRE1α regulates skeletal muscle regeneration through Myostatin mRNA decay. *J. Clin. Invest.* **131**, e143737 (2021).
14. M. A. Pearen, G. E. O. Muscat, Minireview: Nuclear hormone receptor 4A signaling: Implications for metabolic disease. *Mol. Endocrinol.* **24**, 1891–1903 (2010).
15. K. B. Umansky *et al.*, Runx1 transcription factor is required for myoblasts proliferation during muscle regeneration. *PLoS Genet.* **11**, e1005457 (2015).
16. M. Cassandri *et al.*, Zinc-finger proteins in health and disease. *Cell Death Discov.* **3**, 17071 (2017).
17. F. Sarto *et al.*, Effects of short-term unloading and active recovery on human motor unit properties, neuromuscular junction transmission and transcriptomic profile. *J. Physiol.* **600**, 4731–4751 (2022).
18. X. Zhang *et al.*, Impaired mitochondrial energetics characterize poor early recovery of muscle mass following hind limb unloading in old mice. *J. Gerontol., Ser. A, Biol. Sci. Med. Sci.* **73**, 1313–1322 (2018).
19. P. Hettige, U. Tahir, K. C. Nishikawa, M. J. Gage, Transcriptomic profiles of muscular dystrophy with myositis (mdm) in extensor digitorum longus, psoas, and soleus muscles from mice. *BMC Genomics* **23**, 657 (2022).
20. J. G. Tidball, Mechanisms of muscle injury, repair, and regeneration. *Compr. Physiol.* **1**, 2029–2062 (2011).
21. V. E. Baracos, L. Martin, M. Korc, D. C. Guttridge, K. C. H. Fearon, Cancer-associated cachexia. *Nat. Rev. Dis. Primers* **4**, 17105 (2018).
22. T. A. Blackwell *et al.*, Transcriptomic analysis of the development of skeletal muscle atrophy in cancer-cachexia in tumor-bearing mice. *Physiol. Genomics* **50**, 1071–1082 (2018).
23. N. J. Pillon *et al.*, Distinctive exercise-induced inflammatory response and exerkine induction in skeletal muscle of people with type 2 diabetes. *Sci. Adv.* **8**, eabo3192 (2022).
24. M. J. Petrany *et al.*, Single-nucleus RNA-seq identifies transcriptional heterogeneity in multinucleated skeletal myofibers. *Nat. Commun.* **11**, 6374 (2020).
25. A. J. De Micheli *et al.*, Single-cell analysis of the muscle stem cell hierarchy identifies heterotypic communication signals involved in skeletal muscle regeneration. *Cell Rep.* **30**, 3583–3595.e5 (2020).
26. V. Gotea, I. Ovcharenko, DiRE: Identifying distant regulatory elements of co-expressed genes. *Nucleic Acids Res.* **36**, W133–W139 (2008).
27. M. Cheng, M.-H. Nguyen, G. Fantuzzi, T. J. Koh, Endogenous interferon-gamma is required for efficient skeletal muscle regeneration. *Am. J. Physiol. Cell Physiol.* **294**, C1183–1191 (2008).
28. C. Zhang *et al.*, Age-related decline of interferon-gamma responses in macrophage impairs satellite cell proliferation and regeneration. *J. Cachexia Sarcopenia Muscle* **11**, 1291–1305 (2020).

29. E. L. Van Nostrand *et al.*, Robust transcriptome-wide discovery of RNA-binding protein binding sites with enhanced CLIP (eCLIP). *Nat. Methods* **13**, 508–514 (2016).
30. J. Höck *et al.*, Proteomic and functional analysis of Argonaute-containing mRNA-protein complexes in human cells. *EMBO Rep.* **8**, 1052–1060 (2007).
31. Z. Mourelatos *et al.*, miRNPs: A novel class of ribonucleoproteins containing numerous microRNAs. *Genes Dev.* **16**, 720–728 (2002).
32. S. S. Bradrick, M. Gromeier, Identification of gemin5 as a novel 7-methylguanosine cap-binding protein. *PLoS ONE* **4**, e7030 (2009).
33. N. Liu *et al.*, microRNA-206 promotes skeletal muscle regeneration and delays progression of Duchenne muscular dystrophy in mice. *J. Clin. Invest.* **122**, 2054–2065 (2012).
34. A. H. Williams *et al.*, MicroRNA-206 delays ALS progression and promotes regeneration of neuromuscular synapses in mice. *Science* **326**, 1549–1554 (2009).
35. D. P. Bartel, MicroRNAs: Genomics, biogenesis, mechanism, and function. *Cell* **116**, 281–297 (2004).
36. S. Li *et al.*, Requirement for serum response factor for skeletal muscle growth and maturation revealed by tissue-specific gene deletion in mice. *Proc. Natl. Acad. Sci. U.S.A.* **102**, 1082–1087 (2005).
37. A. M. Newman *et al.*, Determining cell type abundance and expression from bulk tissues with digital cytometry. *Nat. Biotechnol.* **37**, 773–782 (2019).
38. X. J. Musacchia, J. M. Steffen, D. R. Deavers, Rat hindlimb muscle responses to suspension hypokinesia/hypodynamia. *Aviat. Space Environ. Med.* **54**, 1015–1020 (1983).
39. F. Chemello *et al.*, Degenerative and regenerative pathways underlying Duchenne muscular dystrophy revealed by single-nucleus RNA sequencing. *Proc. Natl. Acad. Sci. U.S.A.* **117**, 29691–29701 (2020).
40. J. G. Tidball, Regulation of muscle growth and regeneration by the immune system. *Nat. Rev. Immunol.* **17**, 165–178 (2017).
41. P. J. Ferrara *et al.*, Global deletion of CCL2 has adverse impacts on recovery of skeletal muscle fiber size and function and is muscle specific. *J. Appl. Physiol.* **134**, 923–932 (2023).
42. H. Koike, I. Manabe, Y. Oishi, Mechanisms of cooperative cell–cell interactions in skeletal muscle regeneration. *Inflamm. Regen.* **42**, 48 (2022).
43. H. Lu, D. Huang, R. M. Ransohoff, L. Zhou, Acute skeletal muscle injury: CCL2 expression by both monocytes and injured muscle is required for repair. *FASEB J.* **25**, 3344–3355 (2011).
44. C. Zhang *et al.*, Complement C3a signaling facilitates skeletal muscle regeneration by regulating monocyte function and trafficking. *Nat. Commun.* **8**, 2078 (2017).
45. S. Zhuang, A. Russell, Y. Guo, Y. Xu, W. Xiao, IFN-γ blockade after genetic inhibition of PD-1 aggravates skeletal muscle damage and impairs skeletal muscle regeneration. *Cell Mol. Biol. Lett.* **28**, 27 (2023).
46. S. Mahurkar *et al.*, Response to interferon-beta treatment in multiple sclerosis patients: A genome-wide association study. *Pharmacogenomics J.* **17**, 312–318 (2017).
47. N. A. Dumont, C. F. Bentzinger, M.-C. Sincennes, M. A. Rudnicki, Satellite cells and skeletal muscle regeneration. *Compr. Physiol.* **5**, 1027–1059 (2015).
48. M. N. Wosczyna *et al.*, Mesenchymal stromal cells are required for regeneration and homeostatic maintenance of skeletal muscle. *Cell Rep.* **27**, 2029–2035.e5 (2019).
49. S. J. Forbes, N. Rosenthal, Preparing the ground for tissue regeneration: From mechanism to therapy. *Nat. Med.* **20**, 857–869 (2014).
50. C. J. Mann *et al.*, Aberrant repair and fibrosis development in skeletal muscle. *Skelet. Muscle* **1**, 21 (2011).
51. S. Hayashi, I. Manabe, Y. Suzuki, F. Relaix, Y. Oishi, Klf5 regulates muscle differentiation by directly targeting muscle-specific genes in cooperation with MyoD in mice. *eLife* **5**, e17462 (2016).
52. K. Sunadome *et al.*, ERK5 regulates muscle cell fusion through Klf transcription factors. *Dev. Cell* **20**, 192–205 (2011).
53. S. C. Bodine *et al.*, Identification of ubiquitin ligases required for skeletal muscle atrophy. *Science* **294**, 1704–1708 (2001).
54. D. M. S. Ferreira *et al.*, LIM and cysteine-rich domains 1 (LMCD1) regulates skeletal muscle hypertrophy, calcium handling, and force. *Skelet. Muscle* **9**, 26 (2019).
55. J. T. Cunningham *et al.*, mTOR controls mitochondrial oxidative function through a YY1–PGC-1α transcriptional complex. *Nature* **450**, 736–740 (2007).
56. S. M. Haldar *et al.*, Kruppel-like factor 15 regulates skeletal muscle lipid flux and exercise adaptation. *Proc. Natl. Acad. Sci. U.S.A.* **109**, 6739–44 (2012).
57. M. Ha, V. N. Kim, Regulation of microRNA biogenesis. *Nat. Rev. Mol. Cell Biol.* **15**, 509–524 (2014).
58. M. Cesana *et al.*, A long noncoding RNA controls muscle differentiation by functioning as a competing endogenous RNA. *Cell* **147**, 358–369 (2011).
59. S. Khalilian, S. Z. Hosseini Imani, S. Ghafouri-Fard, Emerging roles and mechanisms of miR-206 in human disorders: A comprehensive review. *Cancer Cell Int.* **22**, 412 (2022).
60. E. L. Van Nostrand *et al.*, Principles of RNA processing from analysis of enhanced CLIP maps for 150 RNA binding proteins. *Genome Biol.* **21**, 90 (2020).
61. A. M. Herzner *et al.*, ADAR and hnRNPC deficiency synergize in activating endogenous dsRNA-induced type I IFN responses. *J. Exp. Med.* **218**, e20201833 (2021).
62. W. Zhu *et al.*, Retrotransposon long interspersed nucleotide element-1 (LINE-1) is activated during salamander limb regeneration. *Dev. Growth Differ.* **54**, 673–685 (2012).
63. M. J. Heinrich *et al.*, Endogenous double-stranded Alu RNA elements stimulate IFN-responses in relapsing remitting multiple sclerosis. *J. Autoimmun.* **100**, 40–51 (2019).
64. Y. Kong *et al.*, Transposable element expression in tumors is associated with immune infiltration and increased antigenicity. *Nat. Commun.* **10**, 5228 (2019).
65. J. Liu *et al.*, Molecular characterization of the transition from acute to chronic kidney injury following ischemia/reperfusion. *JCI Insight* **2**, e94716 (2017).
66. W. Liu *et al.*, Pyroptosis inhibition improves the symptom of acute myocardial infarction. *Cell Death Dis.* **12**, 852 (2021).
67. A. H. Guo *et al.*, Sirtuin 5 levels are limiting in preserving cardiac function and suppressing fibrosis in response to pressure overload. *Sci Rep.* **12**, 12258 (2022).
68. T. Yokota *et al.*, Type V collagen in scar tissue regulates the size of scar after heart injury. *Cell* **182**, 545–562.e23 (2020).
69. N. J. Pillon *et al.*, Transcriptomic profiling of skeletal muscle adaptations to exercise and inactivity. *Nat. Commun.* **11**, 470 (2020).
70. J. C. Correia *et al.*, Analysis of skeletal muscle gene expression upon mouse hindlimb unloading and reloading. Gene Expression Omnibus. https://www.ncbi.nlm.nih.gov/geo/query/acc.cgi?acc=GSE237099. Deposited 11 July 2023.
71. J. C. Correia *et al.*, Zfp697 is an RNA-binding protein that regulates skeletal muscle inflammation and remodeling (Zfp697 skeletal muscle knockout RNA-Seq of unloading-reloading protocol). Gene Expression Omnibus. https://www.ncbi.nlm.nih.gov/geo/query/acc.cgi?acc=GSE273092. Deposited 25 July 2024.
72. J. C. Correia *et al.*, Zfp697 is an RNA-binding protein that regulates skeletal muscle inflammation and remodeling (Zfp697 transduced primary mouse myotubes RNA-Seq). Gene Expression Omnibus. https://www.ncbi.nlm.nih.gov/geo/query/acc.cgi?acc=GSE273093. Deposited 25 July 2024.
73. J. C. Correia *et al.*, Zfp697 is an RNA-binding protein that regulates skeletal muscle inflammation and remodeling (Zfp697 transduced primary mouse myotubes ChIP-Seq). Gene Expression Omnibus. https://www.ncbi.nlm.nih.gov/geo/query/acc.cgi?acc=GSE273094. Deposited 25 July 2024.